Frost, Ray L., López, Andrés, Scholz, Ricardo, Sampaio, Ney Pinheiro, & de Oliveira, Fernando A.N.
(2015)
SEM, EDS and vibrational spectroscopic study of dawsonite NaAl(CO3)(OH)2.
Spectrochimica Acta Part A : Molecular and Biomolecular Spectroscopy, *136*(Part B), pp. 918-923.

SEM, EDS and vibrational spectroscopic study of dawsonite $NaAl(CO_3)(OH)_2$

Ray L. Frost [a•], Andrés López[a], Ricardo Scholz[b], Ney Pinheiro Sampaio[c], Fernando A. N. de Oliveira[d]

[a] School of Chemistry, Physics and Mechanical Engineering, Science and Engineering Faculty, Queensland University of Technology, GPO Box 2434, Brisbane Queensland 4001, Australia.

[b] Geology Department, School of Mines, Federal University of Ouro Preto, Campus Morro do Cruzeiro, Ouro Preto, MG, 35,400-00, Brazil

[c] NanoLab, REDEMAT, School of Mines, Federal University of Ouro Preto, Campus Morro do Cruzeiro, Ouro Preto, MG, 35,400-00, Brazil

[d] Federal Institute of Minas Gerais, Campus Ouro Preto, Ouro Preto, MG, 35,400-000, Brazil

Abstract

In this work we have studied the mineral dawsonite by using a combination of scanning electron microscopy with EDS and vibrational spectroscopy. Single crystals show an acicular habitus forming aggregates with a rosette shape. The chemical analysis shows a phase composed of C, Al, and Na. Two distincit Raman bands at 1091 and 1068 cm^{-1} are assigned to the CO_3^{2-} ν_1 symmetric stretching mode. Multiple bands are observed in both the Raman and infrared spectra in the antisymmetric stretching and bending regions showing that the symmetry of the carbonate anion is reduced and in all probablity the carbonate anions are not equivalent in the dawsonite structure. Multiple OH deformation vibrations centred upon 950 cm^{-1} in both the Raman and infrared spectra show that the OH units in the dawsonite structure are non-equivalent. Raman bands observed at 3250, 3283 and 3295 cm^{-1} are assigned to OH stretching vibrations. The position of these bands indicates strong hydrogen bonding of the OH units in the dawsonite structure. The formation of the mineral dawsonite has the potential to offer a mechanism for the geosequestration of greenhouse gases.

• Author to whom correspondence should be addressed (r.frost@qut.edu.au)
P +61 7 3138 2407 F: +61 7 3138 1804

Key words: dawsonite, carbonate, hydroxyl, Infrared and Raman spectroscopy

Introduction

Dawsonite, a sodium aluminium hydroxy carbonate $NaAl(CO_3)(OH)_2$, is orthorhombic with point group mmm (space group no. 74, Imma, Z = 4) and is acicular to bladed crystals and often occurs in rosettes and radial fibrous to tufted aggregates. The mineral dawsonite was discovered by accident during the construction of the Redpath museum on the campus of McGill univeristy on the island of Montreal, Canada [1, 2]. The mineral is formed in a feldspathic dike. The mineral is known from many places world-wide [1, 3-6].

The mineral is formed through low temperature hydrothermal decomposition of aluminous silicates. Varities other than sodium dawsonite are known. Indeed dawsonites with yttrium and cerium are also known [7, 8]. Many of these types of synthetic compounds are used as catalyst precursors. Dawsonite formation is used in water purification for the removal of alumina species [9]. It is possible that this type of mineral can be used to trap carbon dioxide and remove green house gases [10, 11]. It is highly likely that dawsonite formation is important during the formation of greenhouse gas traps [12-18].

The infrared spectra of dawsonite has been published [19-25]. Alumina surfaces have been analysed by FTIR spectroscopy [22]. Some reports of the Raman spectra have been published [20, 23]. The authors have undertaken a previous Raman study of dawsonite [26]. In this work, we include an SEM image of dawsonite and its chemical analysis. X-ray crystallography suggests the mineral has a regular structure. However, the infrared data suggests otherwise. The objective of this research is study further the molecular structure of dawsonite. We wish to add to our fundamental knowledge of the chemistry of the mineral dawsonite. It is important from an environmental and geosequestration point of view to be able to identify the presence of the mineral dawsonite.

Experimental

Samples description and preparation

The dawsonite sample studied in this work originated from Poudrette Quarry, Mont Saint-Hilaire, Québéc, Canada. This is the location of the mineral. The compositions have been reported by Anthony et al. (page 176) [27]. The sample is part of the collection of the Geology Department of the Federal University of Ouro Preto, Minas Gerais, Brazil, with

sample code SAD-046. The sample was gently crushed and the associated minerals were removed under a stereomicroscope Zeiss Stemi DV4 from the Museu de Ciência e Técnica of the Federal University of Ouro Preto. Qualitative and semiquantitative chemical analysis via SEM/EDS were applied to the mineral characterization. .

Scanning electron microscopy (SEM)

Experiments and analyses involving electron microscopy were performed in the NanoLab, REDEMAT, School of Mines, Universidade Federal de Ouro Preto, Ouro Preto, Minas Gerais, Brazil. Dawsonite crystals were coated with a 5nm layer of evaporated carbon. Secondary Electron image was obtained using a TESCAN VEGA 3 equipment. Qualitative and semi-quantitative chemical analyses in the EDS mode were performed with an Oxford spectrometer and was applied to support the mineral characterization.

Raman microprobe spectroscopy

Crystals of dawsonite were placed on a polished metal surface on the stage of an Olympus BHSM microscope, which is equipped with 10x, 20x, and 50x objectives. The microscope is part of a Renishaw 1000 Raman microscope system, which also includes a monochromator, a filter system and a CCD detector (1024 pixels). The Raman spectra were excited by a Spectra-Physics model 127 He-Ne laser producing highly polarized light at 633 nm and collected at a nominal resolution of 2 cm^{-1} and a precision of ± 1 cm^{-1} in the range between 200 and 4000 cm^{-1}. Repeated acquisitions on the crystals using the highest magnification (50x) were accumulated to improve the signal to noise ratio of the spectra. Raman Spectra were calibrated using the 520.5 cm^{-1} line of a silicon wafer. The Raman spectrum of at least 10 crystals was collected to ensure the consistency of the spectra.

An image of the dawsonite crystals measured is shown in the supplementary information as Figure S1. Clearly the crystals of dawsonite are readily observed, making the Raman spectroscopic measurements readily obtainable.

Infrared spectroscopy

Infrared spectra of dawsonite were obtained using a Nicolet Nexus 870 FTIR spectrometer with a smart endurance single bounce diamond ATR cell. Spectra over the 4000–525 cm^{-1} range were obtained by the co-addition of 128 scans with a resolution of 4

cm^{-1} and a mirror velocity of 0.6329 cm/s. Spectra were co-added to improve the signal to noise ratio.

Spectral manipulation such as baseline correction/adjustment and smoothing were performed using the Spectracalc software package GRAMS (Galactic Industries Corporation, NH, USA). Band component analysis was undertaken using the Jandel 'Peakfit' software package that enabled the type of fitting function to be selected and allows specific parameters to be fixed or varied accordingly. Band fitting was done using a Lorentzian-Gaussian cross-product function with the minimum number of component bands used for the fitting process. The Lorentzian-Gaussian ratio was maintained at values greater than 0.7 and fitting was undertaken until reproducible results were obtained with squared correlations of r^2 greater than 0.995.

Results and discussion

Chemical characterization

The SEM image of dawsonite sample studied in this work is shown in Figure 1. The image shows a fragment of a crystal aggregate. Single crystals show an acicular habitus forming aggregates with rosette shape. Quantitative chemical analysis is provided in Figure 2 and shows a phase composed by C, Al, Na. Minor amounts of Cl where also observed.

Vibrational spectroscopy

Spectroscopy of carbonate anion

It is important to understand the vibrational spectroscopy of the carbonate anion in different molecular environments. Nakamoto *et al.* first published and tabulated the selection rules for unidentate and bidentate anions including the carbonate anion [28, 29]. The free ion, CO_3^{2-} with D_{3h} symmetry exhibits four normal vibrational modes; a symmetric stretching vibration (ν_1), an out-of-plane bend (ν_2), a doubly degenerate asymmetric stretch (ν_3) and another doubly degenerate bending mode (ν_4). The symmetries of these modes are A_1' (R) + A_2'' (IR) + E′ (R, IR) + E′′ (R, IR) and occur at 1063, 879, 1415 and 680 cm^{-1} respectively. Generally, strong Raman modes appear around 1100 cm^{-1} due to the symmetric stretching vibration (ν_1), of the carbonate groups, while intense IR and weak Raman peaks near 1400 cm^{-1} are due to the antisymmetric stretching mode (ν_3). Infrared modes near 800 cm^{-1} are derived from the out-of-plane bend (ν_2). Infrared and Raman modes around 700 cm^{-1} region are due to the in-plane bending mode (ν_4). This mode is doubly degenerate for undistorted

CO_3^{2-} groups [29]. As the carbonate groups become distorted from regular planar symmetry, this mode splits into two components [29]. Infrared and Raman spectroscopy provide sensitive test for structural distortion of CO_3^{2}.

Vibrational spectroscopy of dawsonite

The Raman spectrum of dawsonite in the 100 to 4000 cm^{-1} spectral range is displayed in Figure 3a. This spectrum shows the position and relative intensities of the Raman bands. It is noted that there are large parts of the spectrum where no intensity or minimal intensity is observed. Thus, the spectrum is subdivided into subsections depending upon the type of vibration being studied. The infrared spectrum of dawsonite in the 500 to 4000 cm^{-1} spectral region is shown in Figure 3b. This figure shows the position of the infrared bands and their relative intensities. This spectrum displays the position and relative intensities of the infrared bands. As for the Raman spectrum, there are parts of the spectrum where little or no intensity is observed.

The Raman spectrum of dawsonite over the 800 to 1400 cm^{-1} spectral range is illustrated in Figure 4a. The spectral region centred upon 1091 cm^{-1} is complex with a number of overlapping bands. Two distincit bands are observed at 1091 and 1068 cm^{-1} with a shoulder band at 1099 cm^{-1} on the higher wavenumber side. These bands are attributed to the ν_1 symmetric stretching modes. According to Farmer [30] the structure of dawsonite is stated to be quite regular. The structural analysis of dawsonite suggests that the $(CO_3)^{2-}$ ion is regular and is not involved with bonding [1, 31, 32]. This suggestion is not consistent with the Raman spectrum as multiple bands are observed in the $(CO_3)^{2-}$ stretching region. Farmer also reported the ν_1 band to be two quite distinct bands which is unusual for a single $(CO_3)^{2-}$ ion [30]. This observation implies that there are two distinct carbonate units in the dawsonite structure. A very low intensity Raman band is found at 1366 cm^{-1} which is assigned to the ν_3 antisymmetric stretching mode. This band is of a low intensity and it is highly likely to be a multiple component band. The observation of multiple bands supports the concept that the symmetry of the carbonate anion is reduced. Two bands are observed in the Raman spectra for dawsonite at 936 and 898 cm^{-1}. Frueh and Golightly reported two infrared bands at 950 and 930 cm^{-1} and Farmer assigned these bands to OH deformation modes. Thus, the two Raman bands at 898 and 936 cm^{-1} are attributed to the OH deformation bands of dawsonite. Two Raman bands are observed at 820 and 824 cm^{-1} and are attributed to the ν_4 bending mode.

The infrared spectrum of dawsonite over the 650 to 1150 cm^{-1} spectral range is reported in Figure 4b. This figure displays a number of spectral features including the two infrared bands at 1082 and 1097 cm^{-1}, which are attributed to the CO_3^{2-} ν_1 symmetric stretching mode. Such a vibration should not be observed in the infrared spectrum. If the carbonate anion shows some reduction in symmetry, then the vibrational mode will be activated and the band observed in the infrared spectrum. A series of infrared bands are observed at 914, 942 and 955 $cm^{-1}$and are the equivalent of the Raman bands in similar positions and are assigned to hydroxyl deformation modes. In the infrared spectrum, three bands are noted at 844, 847 and 864 cm^{-1} and are assigned to the ν_4 bending mode. The observation of multiple bands in the ν_4 region provides further evidence for the nonequivalence of the carbonate units in the dawsonite structure.

The Raman spectrum of dawsonite over the 300 to 800 cm^{-1} spectral range is shown in Figure 5a. Bands in this figure are well below the position of any carbonate bands. An intense band observed at 590 cm^{-1} and is assigned to an AlO stretching vibration. Frueh and Golightly reported a band at 685 cm^{-1} and assigned the band to this vibrational mode [33]. Serna et al. attributed most of the vibrational bands below 700 cm^{-1} to AlO modes [23]. It is probable that the band at 519 cm^{-1} is also attributable to an AlO symmetric stretching vibration. Two bands are observed at ~361, 374 and 389 cm^{-1} and may be assigned to OAlO bending modes. The Raman spectrum of dawsonite over the 100 to 300 cm^{-1} spectral range is shown in Figure 5b. A number of Raman bands are observed at 134, 152, 188, 191, 219 and 261 cm^{-1}. These bands are defined as external vibrations.

The Raman spectrum of dawsonite over the 2600 to 3800 cm^{-1} spectral region is given in Figure 6a. Raman bands are observed at 3250, 3283 and 3295 cm^{-1} with broad low intensity bands at 3218 and 3341 cm^{-1}. A Raman band in a high wavenumber position is also noted at 3467 cm^{-1}. The infrared spectrum over the 2800 to 3500 cm^{-1} spectral range is reported in Figure 6b. The spectral profile is broad and bands may be resolved at 2995, 3119, 3237, 3279 and 3357 cm^{-1}. The latter two bands are assigned to OH stretching vibrations whilst the remaining bands are ascroibed to water stretching vibrations. Studies have shown a strong correlation between OH stretching frequencies and both O···O bond distances and H···O hydrogen bond distances [34-37]. Libowitzky (1999) showed that a regression function

can be employed relating the hydroxyl stretching frequencies with regression coefficients better than 0.96 using infrared spectroscopy [38]. The function is described as: $\nu_1 = (3592 - 304) \times 109^{\frac{-d(O-O)}{0.1321}}$ cm^{-1}. Thus OH---O hydrogen bond distances may be calculated using the Libowitzky empirical function. The values for the OH stretching vibrations detailed above provide hydrogen bond distances of 2.735 Å (3279 cm^{-1}), 2.7219 Å (3237 cm^{-1}). Frueh and Golightly suggested some hydrogen bonding exists for dawsonite [33]. The values calculated here, support the concept of strong hydrogen bonding between the OH units and the carbonate anions in the dawsonite structure.

Conclusions

This study has shown the structure of dawsonite is not a simple structure as has been proposed based upon X-ray crystallography. Multiple bands are observed in both the Raman and infrared spectra for carbonate anion indicating a symmetry reduction of the carboante anion. An alternative explanation for the observation of mutiple bands is the non-equivalence of the carbonate anions in the dawsonite structure. Multiple bands attributed to the OH deformation modes support the concept of non-equivalent OH units in the dawsonite structure.

The characterisation of carbonate minerals is required to ensure the carbonation pathway of these minerals is completely understood. This study has shown that dawsonite has both carbonate and bicarbonate units. The hydration-carbonation or hydration-and-carbonation reaction path in the NaO-AlO-CO_2-H_2O system at ambient temperature and atmospheric CO_2 is of environmental significance from the standpoint of carbon balance and the removal of green house gases from the atmosphere. The understanding of the thermal stability of the carbonates of aluminium and the relative metastability of hydrous carbonates is extremely important to the sequestration process for the removal of atmospheric CO_2.

Acknowledgements

The financial and infra-structure support of the Discipline of Nanotechnology and Molecular Science, Science and Engineering Faculty of the Queensland University of Technology, is gratefully acknowledged. The Australian Research Council (ARC) is thanked for funding the instrumentation.

References

[1] J.A. Mandarino, D.C. Harris, Can. Min. 8 (1965) 377-381.

[2] E. Corazza, C. Sabelli, S. Vannucci, Neues Jahr. Min.Mt.(1977) 381-397.

[3] M. Blaha, Min. Slov.15 (1983) 570-572.

[4] R. Goldbery, F.C. Loughnan, Amer. Min.55 (1970) 477-490.

[5] R. Goldbery, F.C. Loughnan, Sedimentology, 24 (1977) 565-579.

[6] M.-L.C. Sirbescu, P.I. Nabelek, Amer. Min. 88 (2003) 1055-1059.

[7] J.D. Grice, R.A. Gault, Can. Min. 44 (2006) 105-115.

[8] J.D. Grice, R.A. Gault, A.C. Roberts, M.A. Cooper, Can. Min.38 (2000) 1457-1466.

[9] E. Alvarez-Ayuso, H.W. Nugteren, Water Res. 39 (2005) 2096-2104.

[10] R.L. Frost, S. Bahfenne, J. Graham, J. Raman Spectrosc. 40 (2009) 855-860.

[11] R.L. Frost, S. Bahfenne, J. Graham, W.N. Martens, Thermochim. Acta, 475 (2008) 39-43.

[12] P. Bolourinejad, P. Shoeibi Omrani, R. Herber, Inter. J. Greenhouse Gas Control, 21 (2014) 11-22.

[13] H. Hellevang, P. Aagaard, J. Jahren, Sc.Tech. 4 (2014) 191-199.

[14] J.P. Kaszuba, H.S. Viswanathan, J.W. Carey, Geophys. Res. Let. 38 (2011) L08404/08401-L08404/08405.

[15] A.B. Mitiku, D. Li, S. Bauer, C. Beyer, App. Geochem.36 (2013) 168-186.

[16] J. Tremosa, C. Castillo, C.Q. Vong, C. Kervevan, A. Lassin, P. Audigane, Inter. J. Greenhouse Gas Control, 20 (2014) 2-26.

[17] L. Yang, T. Xu, B. Yang, H. Tian, H. Lei, Geochem. Geophys. Geosystems, 15 (2014) 605-618.

[18] L. Zhao, C.R. Ward, D. French, I.T. Graham, Aus. J. Earth Sc. 61 (2014) 375-394.

[19] P.A. Estep, C. Karr, Jr., Amer. Min.53 (1968) 305-309.

[20] J.V. Garcia-Ramos, C.J. Serna, Revista de la Real Academia de Ciencias Exactas, Fisicas y Naturales de Madrid, 81 (1987) 397-403.

[21] C. Karr, Jr., J.J. Kovach, App. Spectrosc.23 (1969) 219-223.

[22] D.H. Lee, R.A. Condrate Sr, Mat. Let. 23 (1995) 241-246.

[23] C.J. Serna, J.V. Garcia-Ramos, M.J. Pena, Spectrochim. Acta, 41A (1985) 697-702.

[24] C. Su, D.L. Suarez, Clays Clay Min. 45 (1997) 814-825.

[25] D.I. Tsekhovol'skaya, L.Y. Nikolaeva, Nov. Neboksit. Vidy Glinozem. Syr'ya, M., (1982) 231-234.

[26] R.L. Frost, J.M. Bouzaid, J. Raman Spectrosc.38 (2007) 873-879.

[27] J.W. Anthony, R.A. Bideaux, K.W. Bladh, M.C. Nichols, Handbook of Mineralogy, Mineral Data Publishing, Tuscon, Arizona, USA, 2003.

[28] K. Nakamoto, Bunko Kenkyu, 5 (1957) 3-13.

[29] K. Nakamoto, J. Fujita, S. Tanaka, M. Kobayashi, J. Amer. Chem. Soc. 79 (1957) 4904-4908.

[30] V.C. Farmer, Mineralogical Society Monograph 4: The Infrared Spectra of Minerals, 1974.

[31] S.W. Kwon, Taehan Hwahakhoe Chi, 13 (1969) 157-164.

[32] M.N. Smirnov, A.A. Bitner, D.I. Tsekhovol'skaya, L.Y. Nikolaeva, Neboksitovye Vidy Glinozemnogo Syr'ya, (1982) 228-230.

[33] A.J. Frueh, Jr., J.P. Golightly, Can. Min. 9 (1967) 51-56.

[34] J. Emsley, Chem. Soc. Rev.9 (1980) 91-124.

[35] H. Lutz, Struc. Bond. 82 (1995) 85-103.

[36] W. Mikenda, J. Mol. Struc. 147 (1986) 1-15.

[37] A. Novak, Struc. Bond. 18 (1974) 177-216.

[38] E. Libowitsky, Monat. Chem.130 (1999) 1047-1049.

List of figures

Figure 1 - Secondary electron image (SE) of a dawsonite crystal aggregate up to 0.5 mm in length.

Figure 2 - EDS analysis of dawsonite.

Figure 3 (a) Raman spectrum of dawsonite over the 100 to 4000 cm^{-1} spectral range (upper spectrum) (b) Infrared spectrum of dawsonite over the 500 to 4000 cm^{-1} spectral range (lower spectrum)

Figure 4(a) Raman spectrum of dawsonite over the 800 to 1400 cm^{-1} spectral range (upper spectrum) (b) Infrared spectrum of dawsonite over the 650 to 1150 cm^{-1} spectral range (lower spectrum)

Figure 5 (a) Raman spectrum of dawsonite over the 300 to 800 cm^{-1} spectral range (b) Raman spectrum of dawsonite over the 100 to 300 cm^{-1} spectral range

Figure 6 (a) Raman spectrum of dawsonite over the 2600 to 3800 cm^{-1} spectral range (upper spectrum) (b) Infrared spectrum of dawsonite over the 2500 to 3800 cm^{-1} spectral range (lower spectrum)

Figure 7 (a) Raman spectrum of dawsonite over the 1400 to 1800 cm^{-1} spectral range (b) Infrared spectrum of dawsonite over the 1200 to 1700 cm^{-1} spectral range

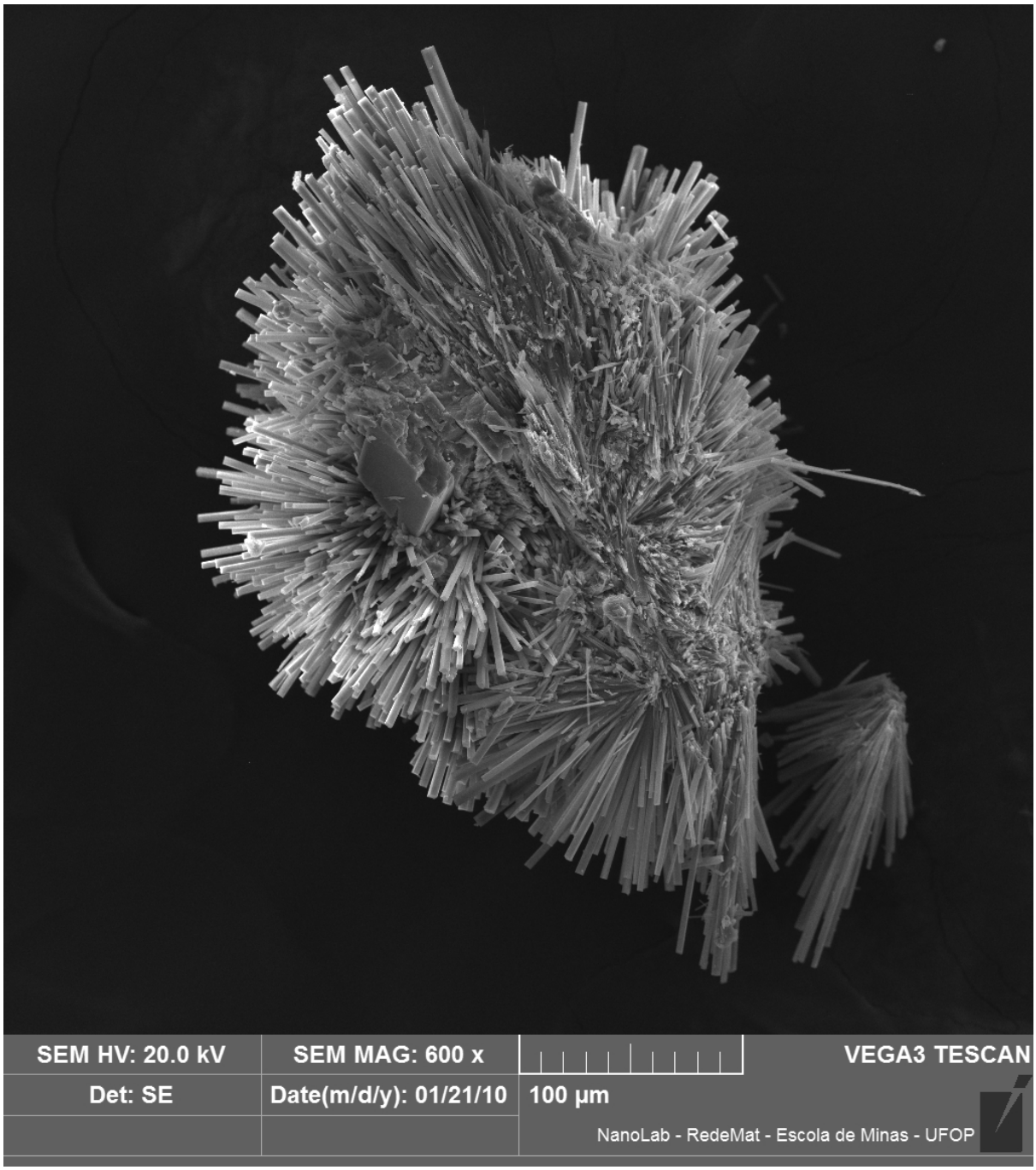

Figure 1 – Secondary electron image (SE) of a dawsonite crystal aggregate up to 0.5 mm in length.

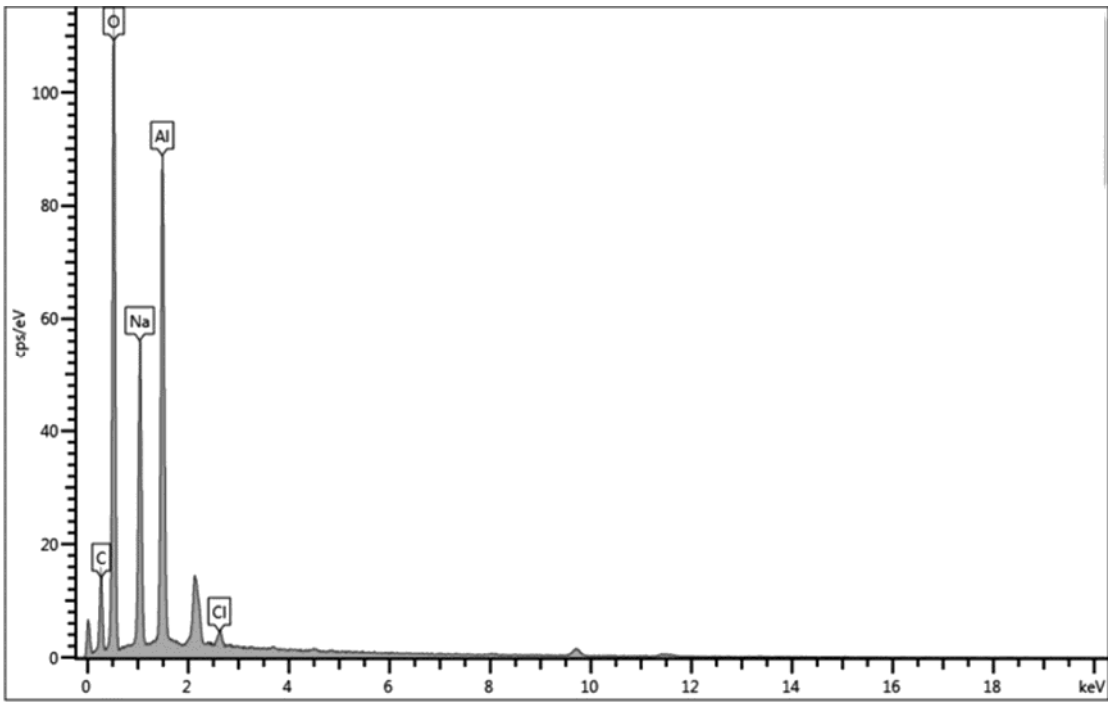

Figure 2 - EDS analysis of dawsonite.

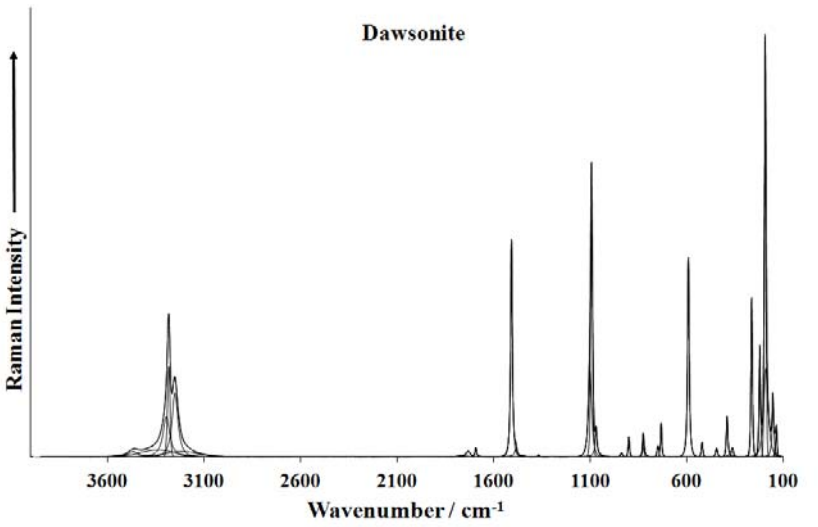

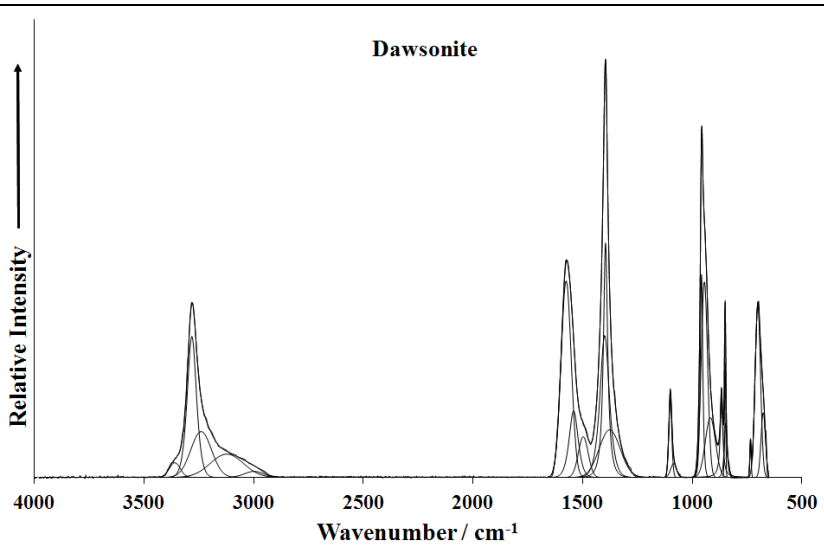

Figure 3 (a) Raman spectrum of dawsonite over the 100 to 4000 cm^{-1} spectral range (upper spectrum) (b) Infrared spectrum of dawsonite over the 500 to 4000 cm^{-1} spectral range (lower spectrum)

335

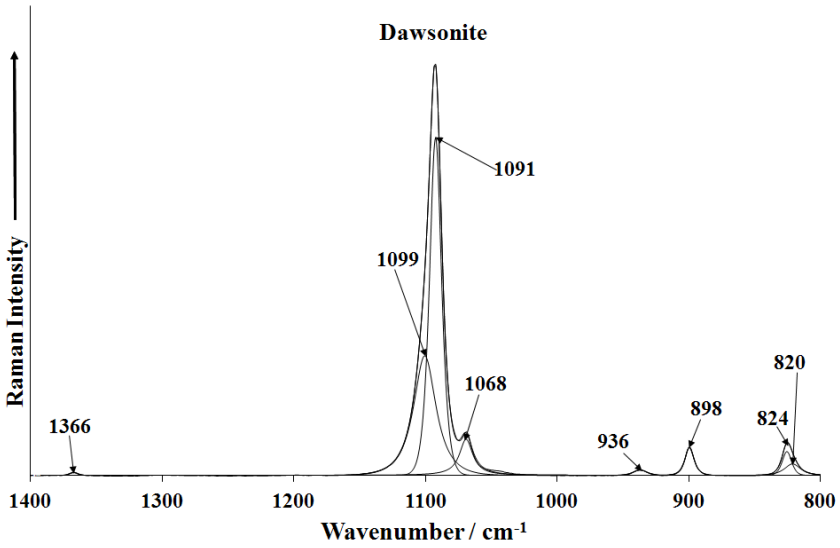

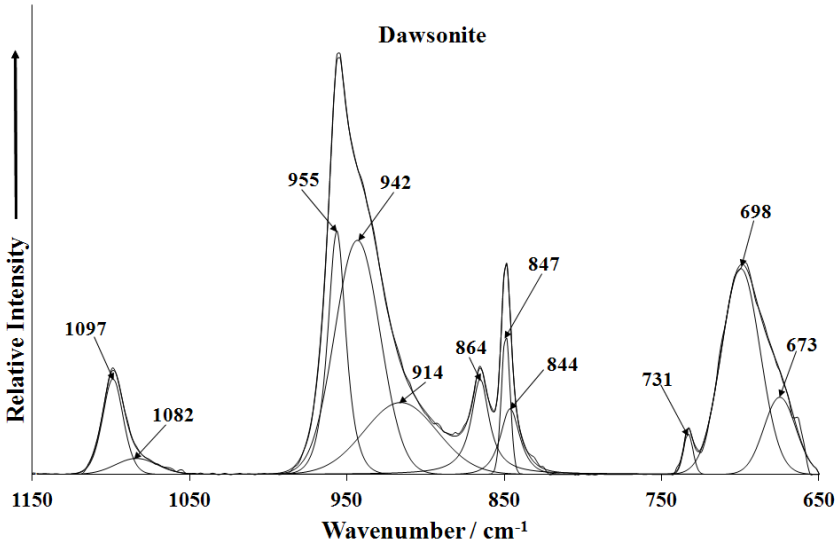

Figure 4a Raman spectrum of dawsonite (upper spectrum) in the 800 to 1400 cm^{-1} spectral range and Figure 4b infrared spectrum of dawsonite (lower spectrum) in the 650 to 1150 cm^{-1} spectral range

336

337

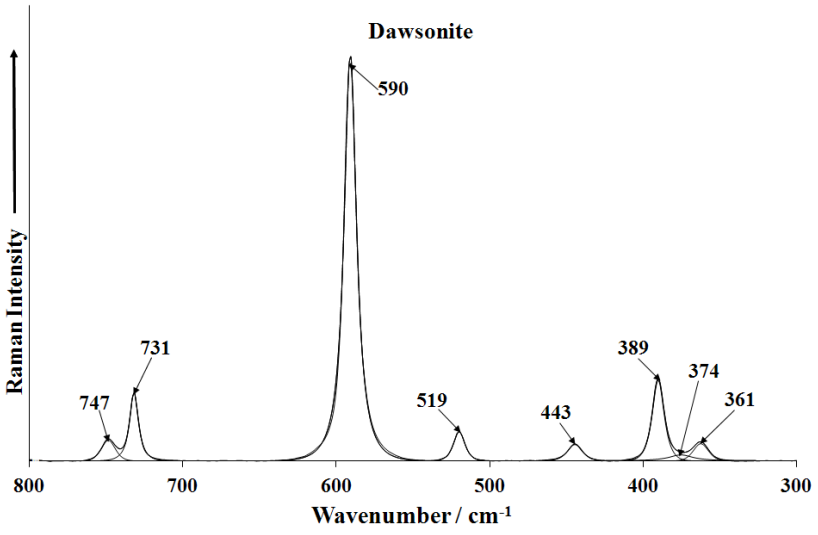

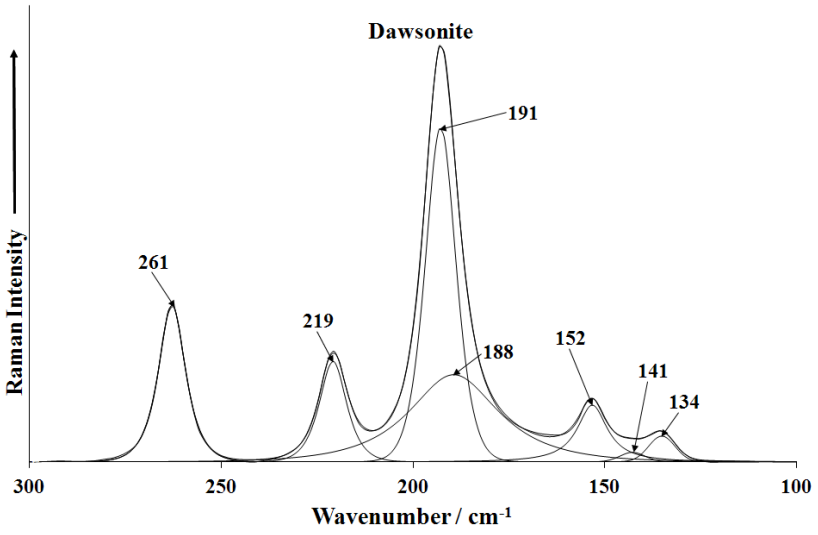

Figure 5a Raman spectrum of dawsonite (upper spectrum) in the 300 to 800 cm^{-1} spectral range and Figure 5b Raman spectrum of dawsonite (lower spectrum) in the 100 to 300 cm^{-1} spectral range

338

339

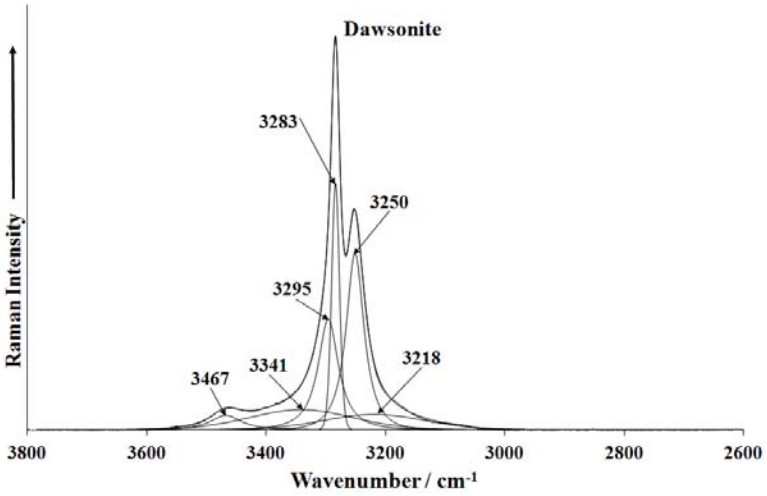

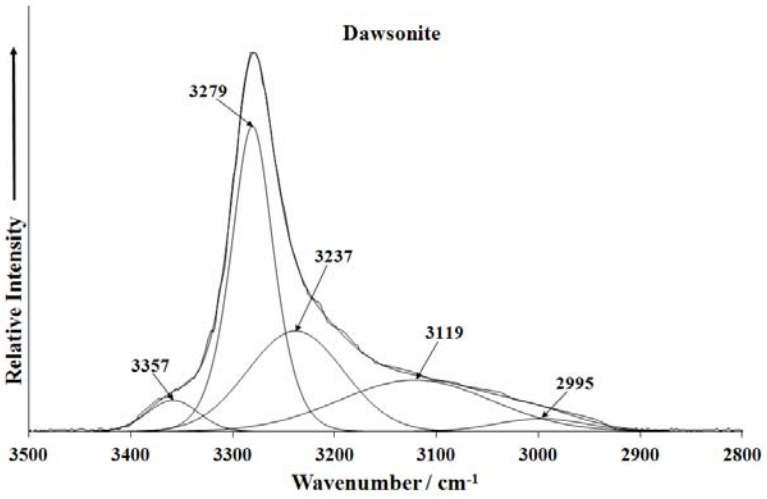

Figure 6a Raman spectrum of dawsonite (upper spectrum) in the 2600 to 3800 cm^{-1} spectral range and Figure 6b infrared spectrum of dawsonite (lower spectrum) in the 2800 to 3500 cm^{-1} spectral range

340

341

342

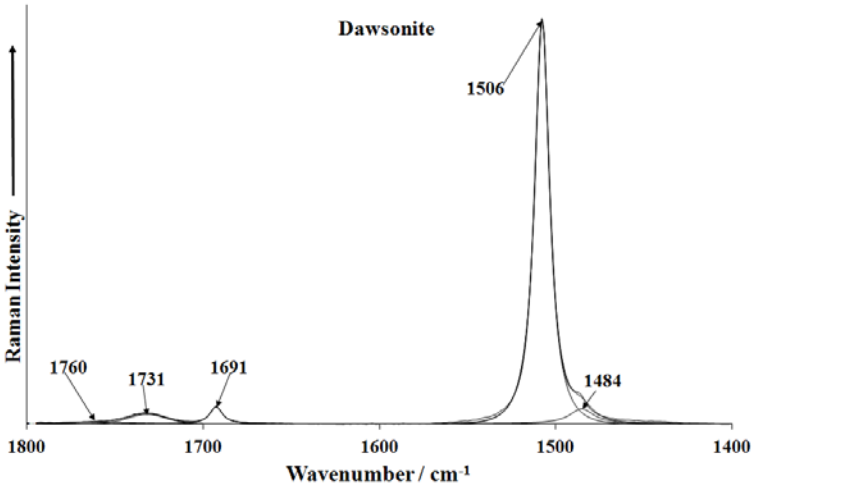

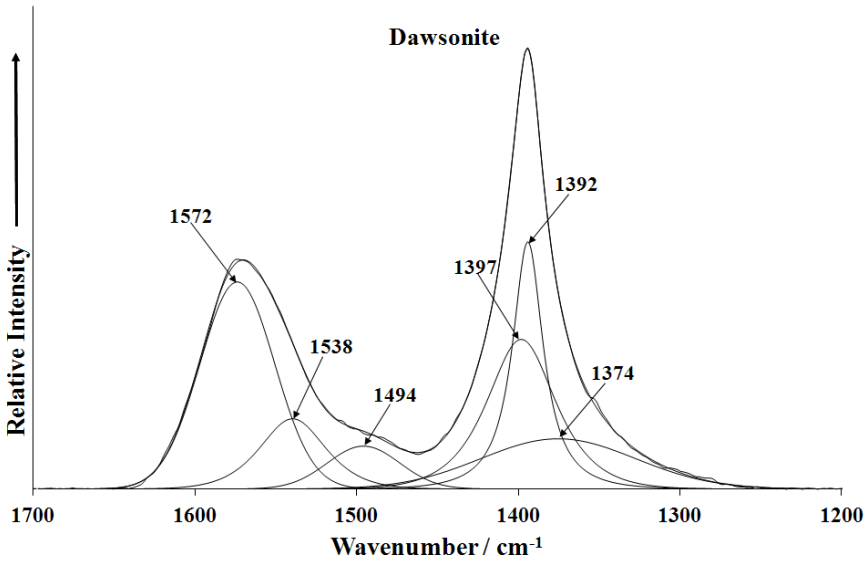

Figure 7a Raman spectrum of dawsonite (upper spectrum) in the 1400 to 1800 cm^{-1} spectral range and Figure 7b infrared spectrum of dawsonite (lower spectrum) in the 1200 to 1700 cm^{-1} spectral range

343

344

345

346